

Kinetic Capillary Electrophoresis (KCE): A Conceptual Platform for Kinetic Homogeneous Affinity Methods

Alexander Petrov, Victor Okhonin, Maxim Berezovski, and Sergey N. Krylov*

*Contribution from the Department of Chemistry, York University,
Toronto, Ontario M3J 1P3, Canada*

Received September 9, 2005; E-mail: skrylov@yorku.ca

Abstract: We propose kinetic capillary electrophoresis (KCE) as a conceptual platform for the development of kinetic homogeneous affinity methods. KCE is defined as the CE separation of species that interact during electrophoresis. Depending on how the interaction is arranged, different KCE methods can be designed. All KCE methods are described by the same mathematics: the same system of partial differential equations with only initial and boundary conditions being different. Every qualitatively unique set of initial and boundary conditions defines a unique KCE method. Here, we (i) present the theoretical bases of KCE, (ii) define four new KCE methods, and (iii) propose a multimethod KCE toolbox as an integrated kinetic technique. Using the KCE toolbox, we were able to, for the first time, observe high-affinity (specific) and low-affinity (nonspecific) interactions within the same protein–ligand pair. The concept of KCE allows for the creation of an expanding toolset of powerful kinetic homogeneous affinity methods, which will find their applications in studies of biomolecular interactions, quantitative analyses, and selecting affinity probes and drug candidates from complex mixtures.

Introduction

Affinity methods play a crucial role in modern life sciences. In addition to affinity purification, their applications include quantitative analyses of biomolecules,¹ studies of biomolecular interactions,² and selection of affinity probes and drug candidates from complex mixtures, such as combinatorial libraries.³ Conceptually, all affinity methods are based on noncovalent binding of a ligand (L) and a target (T) with the formation of a ligand–target complex (C):



where k_{on} and k_{off} are rate constants of complex formation and dissociation, respectively. The stability of C is typically described in terms of the equilibrium dissociation constant, $K_d = k_{\text{off}}/k_{\text{on}}$.

This work is concerned with separation-based affinity methods, which are based on the physical separation of free L from C. Depending on how the separation is carried out, these methods can be classified as heterogeneous or homogeneous. In heterogeneous methods,⁴ T is affixed to a solid substrate, while L is dissolved in a solution. The complexes are formed on the surface while free L remains in solution, thus allowing

for separation of L from C. Heterogeneous methods often suffer from nonspecific binding of L to the surface and changes in the affinity caused by the immobilization of T.⁵ In homogeneous methods, both T and L are dissolved and the complexes are formed in a solution.⁶ Separation of L from C is then achieved based on differences in the mobility of L and C in the homogeneous phase (e.g., by electrophoresis).

Separation-based affinity methods can also be classified as kinetic or nonkinetic. Kinetic methods are those that do not assume equilibrium in reaction 1 and can thus be used for (i) quantitative affinity analyses with “weak” affinity probes (high k_{off}), (ii) measuring k_{on} and k_{off} , and (iii) selection of binding ligands with predetermined k_{on} and k_{off} . Nonkinetic methods, in contrast, assume equilibrium and, thus, cannot serve for these tasks. The assumption of equilibrium in nonkinetic methods is not conceptually required; moreover, equilibrium cannot be maintained in separation-based affinity methods. Thus, all nonkinetic methods can be converted to kinetic methods by changing conditions and approaches for data analysis.

In general, homogeneous methods are preferable due to their simplicity and kinetic methods are preferable due to their enabling kinetic features. Until recently, the only method with comprehensive kinetic capabilities was surface plasmon resonance (SPR), a heterogeneous method.⁷ We introduced the first two separation-based homogeneous methods with comprehensive kinetic capabilities: nonequilibrium capillary electrophore-

(1) Okerberg, E. S.; Wu, J.; Zhang, B.; Samii, B.; Blackford, K.; Winn, D. T.; Shreder, K. R.; Burbaum, J. J.; Patricelli, M. P. *Proc. Natl. Acad. Sci. U.S.A.* **2005**, *102*, 4996–5001.

(2) Licitra, E. J.; Liu, J. O. *Proc. Natl. Acad. Sci. U.S.A.* **1996**, *93*, 12817–12821.

(3) Tuerk, C.; Gold, L. *Science* **1990**, *249*, 505–510.

(4) Woodbury, C. P., Jr.; Venton D. L. *J. Chromatogr., B* **1999**, *725*, 113–137.

(5) Mitchell, P. *Nat. Biotechnol.* **2002**, *20*, 225–229.

(6) Cooper, M. A. *J. Mol. Recognit.* **2004**, *17*, 286–315.

(7) Wilson, W. D. *Science* **2002**, *295*, 2103–2105.

sis of equilibrium mixtures (NECEEM)⁸ and sweeping capillary electrophoresis (SweepCE).⁹ The spectrum of their applications already includes (i) measuring k_{on} , K_{d} , and k_{off} ,^{8–13} (ii) quantitative affinity analyses of proteins,^{12–14} (iii) measuring the temperature inside the capillary,¹⁵ (iv) studying the thermochemistry of affinity interactions,¹⁶ and (v) kinetic selection of ligands from combinatorial libraries.¹⁷ This work was inspired by the insight that NECEEM and SweepCE are based on the same conceptual platform, which we call kinetic capillary electrophoresis (KCE). It was further driven by the idea that the concept of KCE can be used to design new kinetic homogeneous affinity methods.

Results

Theoretical Basis of KCE. We define KCE as the CE separation of species that interact during electrophoresis. Thus, KCE involves two major processes: affinity interaction of L and T, described by eq 1, and separation of L, T, and C based on differences in their electrophoretic velocities, v_{L} , v_{T} , and v_{C} . These two processes are described by the following general system of partial differential equations:

$$\frac{\partial L(t,x)}{\partial t} + v_{\text{L}} \frac{\partial L(t,x)}{\partial x} = -k_{\text{on}}L(t,x)T(t,x) + k_{\text{off}}C(t,x) \quad (2)$$

$$\frac{\partial T(t,x)}{\partial t} + v_{\text{T}} \frac{\partial T(t,x)}{\partial x} = -k_{\text{on}}L(t,x)T(t,x) + k_{\text{off}}C(t,x)$$

$$\frac{\partial C(t,x)}{\partial t} + v_{\text{C}} \frac{\partial C(t,x)}{\partial x} = -k_{\text{off}}C(t,x) + k_{\text{on}}L(t,x)T(t,x)$$

where L , T , and C are the concentrations of L, T, and C, respectively; t is the time passed since the beginning of separation; x is the distance from the injection end of the capillary. System 2 describes the two basic processes, which are always present in KCE. Depending on the species studied and a specific analytical setup, other processes, such as binding with complex stoichiometry, diffusion, adsorption to capillary walls, etc., can play significant roles in KCE. In such cases, mathematical terms, describing additional processes, must be added to system 2. The solution of system 2 depends on the initial and boundary conditions: initial distribution of L, T, and C along the capillary and the way L, T, and C are introduced into the capillary and removed from the capillary during separation. This solution can be found nonnumerically for specific sets of initial and boundary conditions and specific assumptions.^{10,18} For KCE to be a generic approach, it is required that system 2 be solved for any set of conditions; such solutions can be found only numerically.

Multigrid Algorithm for Numerical Modeling of KCE. In general, numerical simulation of electrophoresis is challenging. The difficulties are associated with the incompatibility of a single “space” grid with different velocities of separated species, whose electrophoretic peaks may have sharp fronts. All conventional methods of electrophoretic simulations rely on using a single grid for x , $x = n\Delta x$, where Δx is the length of the x increment and n is an integer representing the point number in calculations. The grid is usually associated with the velocity, v , of one of the separated species: $x = \Delta x + v\Delta t$, where Δt is the time increment. As a result, the species, which migrate with velocities different from v , are simulated “out of the grid”. This leads to rounding errors that are severely aggravated by sharp fronts of electrophoretic peaks.^{19,20} We addressed this problem by adopting the multigrid approach, which was successfully used in other areas of physical sciences.^{21–23} We designed a multigrid algorithm for solving system 2 with an individual Δx for every one of the three components:

$$\Delta x_{\text{L}} = v_{\text{L}}\Delta t \quad (3)$$

$$\Delta x_{\text{T}} = v_{\text{T}}\Delta t$$

$$\Delta x_{\text{C}} = v_{\text{C}}\Delta t$$

The multigrid algorithm was then used to write a computer program, which calculated $L(t,x)$, $T(t,x)$, and $C(t,x)$. These dependencies could be used to build simulated electropherograms, which could be compared with experimental ones.

We examined the correctness of the multigrid algorithm and the program using two previously introduced methods, NECEEM and SweepCE. Detailed mathematical models of both NECEEM and SweepCE have been recently developed by us using nonnumerical approaches.^{9,18} In addition, Fang and Chen modeled our NECEEM data using the finite difference scheme method (numerical approach).²⁰ Here, we compared simulated NECEEM and SweepCE electropherograms obtained with the numerical multigrid approach developed in this work with those obtained by the nonnumerical approaches developed in our previous works.^{9,18} The electropherograms obtained by numerical and nonnumerical methods were identical confirming the validity of the multigrid algorithm and the computer program based on it. The multigrid approach provides a new powerful tool for modeling chromatographic and electrophoretic data. It tolerates sharp fronts of peaks typical for chromatograms and electropherograms and increases the speed of calculations.

KCE Methods. We state that every set of qualitatively unique initial and boundary conditions for system 2 defines a unique KCE method. Table 1 compares 6 KCE methods: NECEEM, SweepCE, and the four new methods. The following unique and descriptive names were given to the new methods: continuous NECEEM (cNECEEM), short SweepCE (sSweepCE), plug–plug KCE (ppKCE), and short SweepCE of equilibrium mixtures (sSweepCEEM). The new methods were defined by arbitrarily selecting new qualitatively different sets of initial and boundary conditions. The table contains drawings, which

(8) Berezovski, M.; Krylov, S. N. *J. Am. Chem. Soc.* **2002**, *124*, 13674–13675.

(9) Okhonin, V.; Berezovski, M.; Krylov, S. N. *J. Am. Chem. Soc.* **2004**, *126*, 7166–7167.

(10) Krylov, S. N.; Berezovski, M. *Analyst* **2003**, *128*, 571–575.

(11) Yang, P.; Whelan, R. J.; Jameson, E. E.; Kurzer, J. H.; Argetsinger, L. S.; Carter-Su, C.; Kabir, A.; Malik, A.; Kennedy, R. T. *Anal. Chem.* **2005**, *77*, 2482–2489.

(12) Berezovski, M.; Nutiu, R.; Li, Y.; Krylov, S. N. *Anal. Chem.* **2003**, *75*, 1382–1386.

(13) Huang, C.-C.; Cao, Z.; Chang, H.-T.; Tan, W. *Anal. Chem.* **2004**, *76*, 6973–6981.

(14) Berezovski, M.; Krylov, S. N. *J. Am. Chem. Soc.* **2003**, *125*, 13451–13454.

(15) Berezovski, M.; Krylov, S. N. *Anal. Chem.* **2004**, *76*, 7114–7117.

(16) Berezovski, M.; Krylov, S. N. *Anal. Chem.* **2005**, *77*, 1526–1523.

(17) Berezovski, M.; Drabovich, A.; Krylova, S. M.; Mushev, M.; Okhonin, V.; Petrov, A.; Krylov, S. N. *J. Am. Chem. Soc.* **2005**, *127*, 3165–3171.

(18) Okhonin, V.; Krylova, S. M.; Krylov, S. N. *Anal. Chem.* **2004**, *76*, 1507–1512.

(19) Ermakov, S.; Mazhorova, O.; Popov, Y. *Informatica* **1992**, *3*, 173–197.

(20) Fang, N.; Chen, D. D. Y. *Anal. Chem.* **2005**, *77*, 849–847.

(21) Yao, Y. F.; Thomas, T. G.; Sandham, N. D.; Williams, J. J. R. *Theor. Comput. Fluid Dyn.* **2001**, *14*, 337–358.

(22) Liao, C.; Liu, Z.; Zheng, X.; Liu, C. *Combust. Sci. Technol.* **1996**, *119*, 219–260.

(23) Nestler, B. J. *Cryst. Growth* **2005**, *275*, e273–e278.

Table 1. Summary of KCE Methods

KCE method	Schematic representation of initial and boundary conditions	Initial Conditions ^a	Boundary conditions	Simulated concentration profiles
NECEEM		$T(0, x) = \tilde{T}\theta(x)\theta(l-x)$ $L(0, x) = \tilde{L}\theta(x)\theta(l-x)$ $C(0, x) = \tilde{C}\theta(x)\theta(l-x)$ $K_d = \tilde{T}\tilde{L}/\tilde{C}$	$T(t, 0) = 0$ $L(t, 0) = 0$ $C(t, 0) = 0$	
SweepCE		$T(0, x) = \tilde{T}$ $L(0, x) = 0$ $C(0, x) = 0$	$T(t, 0) = \tilde{T}$ $L(t, 0) = 0$ $C(t, 0) = 0$	
cNECEEM (new)		$T(0, x) = 0$ $L(0, x) = 0$ $C(0, x) = 0$	$T(t, 0) = \tilde{T}$ $L(t, 0) = \tilde{L}$ $C(t, 0) = \tilde{C}$ $K_d = \tilde{T}\tilde{L}/\tilde{C}$	
sSweepCE (new)		$T(0, x) = \tilde{T}\theta(x)\theta(l-x)$ $L(0, x) = \tilde{L}\theta(x-l)$ $C(0, x) = 0$	$T(t, 0) = 0$ $L(t, 0) = 0$ $C(t, 0) = 0$	
ppKCE (new)		$T(0, x) = \tilde{T}\theta(x)\theta(l_\tau - x)$ $L(0, x) = \tilde{L}\theta(x-l_\tau) \times \theta(l_\tau + l_L - x)$ $C(0, x) = 0$	$T(t, 0) = 0$ $L(t, 0) = 0$ $C(t, 0) = 0$	
sSweepCEEM (new)		$T(0, x) = \tilde{T}\theta(x)\theta(l-x) + \tilde{T}_2\theta(x-l)$ $L(0, x) = \tilde{L}\theta(x-l)$ $C(0, x) = \tilde{C}\theta(x-l)$ $K_d = \tilde{T}_2\tilde{L}/\tilde{C}$	$T(t, 0) = 0$ $L(t, 0) = 0$ $C(t, 0) = 0$	

^a \tilde{T} , \tilde{L} , and \tilde{C} are initial concentrations of the target, ligand, and the complex, respectively, in solutions or in the equilibrium mixture (EM), l is the length of the corresponding injected plug, and $\theta(x)$ is a function which equals to 1 when $x > 0$ and equals to 0 when $x < 0$.

schematically illustrate initial and boundary conditions as well as showing the mathematical representation of initial and boundary conditions. It also contains representative functions $L(t)$, $T(t)$, and $C(t)$ for a fixed x for each method. The notion of “equilibrium mixture” refers to the mixture of L, T, and C at equilibrium, typically prepared outside the capillary. The concentrations of the three components, \tilde{T} , \tilde{L} , and \tilde{C} , in the equilibrium, mixture are interconnected through the equilibrium dissociation constant, K_d , as $K_d = (\tilde{T}\tilde{L})/\tilde{C}$. As an example, we assume that $v_T > v_L$.

In NECEEM, a short plug of the equilibrium mixture is injected into the inlet of the capillary, which is prefilled with the run buffer. Separation is carried out with both inlet and outlet

reservoirs containing the run buffer only. C continuously dissociates during electrophoresis. If separation is efficient, reassociation of T and L can be neglected. The resulting concentration profiles (time dependencies of concentrations for a fixed x) contain three peaks of T, C, and L and two exponential “smears” of L and T, which occur from the dissociation of C.

In SweepCE, the capillary is filled with L, while the inlet reservoir contains T and the outlet reservoir contains a run buffer. During electrophoresis, T continuously moves through L, causing continuous binding of T to L. Although binding is a prevalent process in SweepCE, dissociation of C can also contribute to the resulting concentration profiles, which contain a single peak of C and plateaus of T and L.

In cNECEEM, the inlet reservoir is filled with the equilibrium mixture while the capillary and the outlet reservoir contain the run buffer. During electrophoresis, C is separated from T, which moves faster, and from L, which moves slower. As a result, C continuously dissociates inside the capillary. Although dissociation is a prevalent process in cNECEEM, reassociation can also contribute to the resulting concentration profiles, which are represented by smooth functions of $T(t)$, $L(t)$, and $C(t)$ with no pronounced peaks.

In sSweepCE, a short plug of T is injected into the capillary prefilled with L. Both inlet and outlet reservoirs contain the run buffer. T moves through L during electrophoresis causing both association of T and L and dissociation of resulting C to occur. The concentration profiles of T and C are peaklike, while that of L is a smooth function.

In ppKCE, the plugs of L and T are injected into the capillary prefilled with the run buffer. The inlet and outlet reservoirs contain the run buffer as well. During electrophoresis T moves through L causing the formation of L. When the zone of T passes L, C starts to dissociate. ppKCE can be considered as a functional hybrid of NECEEM and sSweepCE. The resulting concentration profiles resemble those of NECEEM with a smaller peak of C and “smears” of T and L.

In sSweepCEEM, a short plug of T is injected into the capillary prefilled with the equilibrium mixture. Both inlet and outlet reservoirs contain the run buffer. During electrophoresis, an intricate interplay of dissociation of C and association of T and L occur resulting in sophisticated concentration profiles, which contain peaks and plateaus.

The extents of complex formation and dissociation differ in different KCE methods. KCE methods, therefore, have different accuracies of determination of k_{on} and k_{off} . For example, in NECEEM, complex dissociation prevails over complex formation, thus, making it more “sensitive” to k_{off} than k_{on} . In SweepCE, in contrast, complex formation can prevail over complex dissociation, making it more sensitive to k_{on} than k_{off} . The plug–plug KCE method can be tuned to have comparable accuracy of both k_{on} and k_{off} determination (we are currently working on developing simple mathematics for this method which will allow the calculation of k_{on} and k_{off} using algebraic formulas without nonlinear regression analysis). KCE methods, which involve equilibrium mixtures (e.g., NECEEM, cNECEEM, and sSweepCEEM), are expected to be more accurate for the determination of the equilibrium constant, K_{d} . The most accurate determination of all constants can be achieved if multiple KCE methods are combined in a single kinetic tool (see the next section).

With the use of the general concept of KCE, other KCE methods can be defined by simply selecting new sets of initial and boundary conditions. Importantly, this approach requires no serendipity but, rather, a rational (or irrational) design of conditions, which can be performed in an intuitive way schematically depicted in Table 1.

KCE methods have a wide dynamic range for measuring kinetic and equilibrium constants. The upper limit of K_{d} values is defined by the highest concentration of T available in solution. The lower limit of K_{d} depends on the concentration limit of detection of a CE instrument. For laser-induced fluorescence detection, it can be as low as picomolar. The dynamic range of k_{off} values is defined by the migration time of the complex,

which can be easily controlled by the length of the capillary, electric field, or electroosmotic velocity. The practically proven dynamic range of k_{off} spans from 10^{-4} to 1 s^{-1} .^{8–11} The dynamic range of measurable k_{on} is dependent on the range of applicable concentrations and separation times.⁹ The upper limit of k_{on} is defined by the concentration detection limit of a CE instrument ($\sim 10^{-12} \text{ M}$) and the best time resolution ($\sim 1 \text{ s}$) and equals to $\sim 10^{12} \text{ M}^{-1} \text{ s}^{-1}$. This exceeds the diffusion-controlled limit in solutions by at least 2 orders of magnitude. The lower limit of k_{on} is defined by the highest applicable concentration ($\sim 10^{-3} \text{ M}$) and longest retention time in the capillary ($\sim 10^3 \text{ s}$) and can be estimated as $\sim 1 \text{ M}^{-1} \text{ s}^{-1}$. We recently introduced a new method for mixing solutions inside the capillary; the method is termed transverse diffusion of laminar flow profiles (TDLFP).²⁴ If TDLFP is combined with KCE, only nanoliter volumes of reactants are required.

An important advantage of KCE is its conceptual abstraction from reactions on the surface. In contrast to chromatography, CE does not rely on the interaction with the surface to separate species; therefore, such an interaction is not necessarily included in KCE. Certain molecules (e.g., proteins) can adhere to bare silica of the inner capillary wall, which leads to characteristic peak tailing. Absorption of molecules on the inner capillary wall can be included in the model of KCE as an additional term in system 2. It is more practical, however, to minimize such interaction to the level at which it can be neglected. Absorption of molecules on the capillary wall can be reduced by changing the composition and pH of the run buffer or through coating the inner capillary wall with an “antiadhesive” layer.

Multimethod KCE Toolbox. Here we introduce the simultaneous use of multiple KCE methods as an integrated tool for kinetic studies of biomolecular interactions. The approach can be used for testing hypotheses about the mechanisms of interaction and finding kinetic parameters of the interaction. Conceptually, experimental electropherograms are obtained by multiple KCE methods first. A hypothetical model of interactions between L and T is suggested and the system of differential equations (system 2) is built. The experimental KCE electropherograms are fitted with simulated electropherograms simultaneously to obtain the best fits with one of the criteria used for nonlinear regression analysis (e.g., minimum chi-square). If the quality of fitting is not satisfactory, a new hypothesis is suggested for the interaction. The procedure is repeated until a satisfying hypothesis is found. The best fits for the accepted hypothesis lead to the determination of stoichiometric and kinetic parameters of the interaction. Figure 2 summarizes the general approach to the development and analytical utilization of a multimethod KCE toolbox.

We tested this approach using the six KCE methods depicted in Table 1 and a well-studied experimental system: the interaction between ssDNA-binding protein (SSB) and ssDNA.^{8–10,25,26} Since the velocity of SSB in electrophoresis is greater than that of ssDNA, we assign L to ssDNA and T to SSB. Only L was fluorescently labeled in our study, so that T was not detectable while both L and C were detectable but optically indistinguishable. Simulated electropherograms, there-

- (24) Okhonin, V.; Liu, X.; Krylov, S. N. *Anal. Chem.* **2005**, *77*, 5925–5929.
(25) Hagmar, P.; Dahlman, K.; Takahashi, Mi.; Carlstedt-Duke, J.; Gustafsson, J. A.; Norden, B. *FEBS Lett.* **1989**, *253*, 28–52.
(26) Ferrari, M. E.; Bujalowski, W.; Lohman, T. M. *J. Mol. Biol.* **1994**, *236*, 106–123.

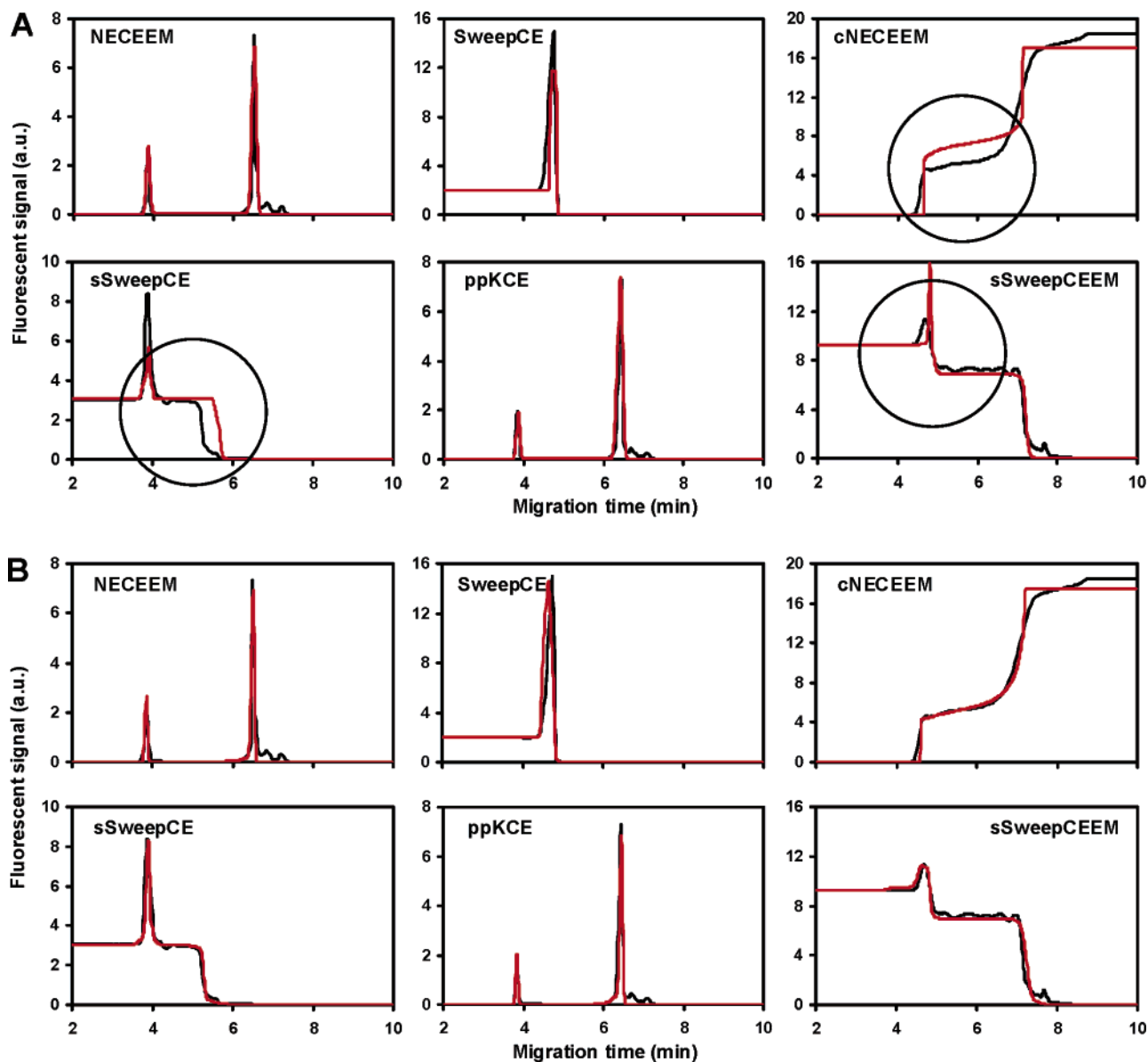


Figure 1. Application of the KCE toolbox to (i) testing hypotheses about the nature of biomolecular interactions and (ii) finding rate constants of interactions. Black traces show experimental electropherograms for six KCE methods, while red traces show simulated electropherograms corresponding to the best fitting using the minimum chi-square criterion. Experimental electropherograms are identical in both panels; simulated electropherograms differ in panels A and B. Panel A presents simulated electropherograms for the unsatisfactory model, which assumes one type of interaction only (eq 1). Circles indicate areas of fitting with unacceptably great deviations between experimental and simulated electropherograms. Panel B shows simulated electropherograms for the satisfying model, which assumes two types of interactions (eq 4). Rate constants obtained by fitting with the satisfying model are shown in expression 6.

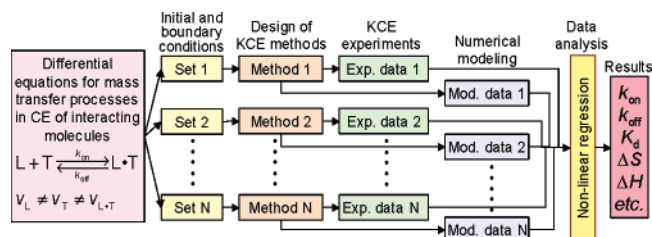


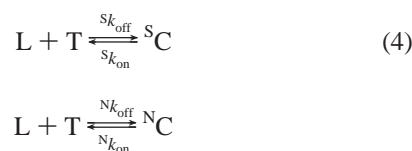
Figure 2. Flowchart depicting the general approach to the development and utilization of a multimethod KCE toolbox.

fore, were calculated as dependencies of $L(t) + C(t)$ for x equal to the distance from the injection end of the capillary to the detector. Such simulated electropherograms could be directly compared with experimental ones.

We first tested a hypothesis that SSB and DNA interaction is described by eq 1. The best fit of six experimental KCE electropherograms for this hypothesis was obtained for $k_{\text{on}} = 6 \times 10^6 \text{ M}^{-1} \text{ s}^{-1}$ and $k_{\text{off}} = 9 \times 10^{-4} \text{ s}^{-1}$ (Figure 1A.). Deviations between experimental and simulated electropherograms were unacceptably high for cNECEEM, sSweepCE, and sSweepCEEM thus suggesting that hypothesis 1 was not valid.

Second, we modified the hypothesis based on existing empirical data about the SSB–ssDNA interaction. Two types of interactions have been previously hypothesized for SSB and ssDNA: high-affinity specific binding and low-affinity non-specific binding.^{25,26} Nonspecific binding was hypothesized to occur due to electrostatic attraction between SSB and DNA, which does not necessarily involve the DNA-binding site of

SSB. To account for two types of binding we modified reaction 1 to include two types of complexes and two sets of rate constants:



where “S” and “N” denote specific and nonspecific interactions, respectively. The system of differential equations similar to that of system 2 was built for model 4:

$$\frac{\partial L(t,x)}{\partial t} + v_L \frac{\partial L(t,x)}{\partial x} = -(S_{k_{\text{on}}} + N_{k_{\text{on}}})L(t,x)T(t,x) + S_{k_{\text{off}}} S C + N_{k_{\text{off}}} N C \quad (5)$$

$$\frac{\partial T(t,x)}{\partial t} + v_T \frac{\partial T(t,x)}{\partial x} = -(S_{k_{\text{on}}} + N_{k_{\text{on}}})L(t,x)T(t,x) + S_{k_{\text{off}}} S C + N_{k_{\text{off}}} N C$$

$$\frac{\partial S C(t,x)}{\partial t} + v_C \frac{\partial S C(t,x)}{\partial x} = -S_{k_{\text{off}}} S C + S_{k_{\text{on}}} L(t,x)T(t,x)$$

$$\frac{\partial N C(t,x)}{\partial t} + v_C \frac{\partial N C(t,x)}{\partial x} = -N_{k_{\text{off}}} N C + N_{k_{\text{on}}} L(t,x)T(t,x)$$

Experimental KCE electropherograms were then fitted with simulated ones for the new model. The best fit was found to be in acceptable quantitative agreement with the experimental data (Figure 1B), which allowed us to accept model 4. The values of rate constants obtained from the nonlinear regression analysis were as follows:

$$S_{k_{\text{on}}} = 5 \times 10^5 \text{ M}^{-1} \text{ s}^{-1} \quad (6)$$

$$S_{k_{\text{off}}} = 6 \times 10^{-4} \text{ s}^{-1}$$

$$N_{k_{\text{on}}} = 8 \times 10^6 \text{ M}^{-1} \text{ s}^{-1}$$

$$N_{k_{\text{off}}} = 8 \times 10^{-2} \text{ s}^{-1}$$

The determined sets of rate constants well fit the definition of specific and nonspecific interactions. Specific binding requires a specific orientation of molecules during binding, while nonspecific binding occurs independently of the orientation. Accordingly, $S_{k_{\text{on}}}$ is an order of magnitude lower than $N_{k_{\text{on}}}$. When specific binding occurs, it is more stable than nonspecific. Accordingly $S_{k_{\text{off}}}$ is 2 orders of magnitude below $N_{k_{\text{off}}}$. As a result, the equilibrium dissociation constant for specific interactions, $S_{K_d} = 1.2 \times 10^{-9} \text{ M}$, is an order of magnitude lower than that of nonspecific interactions, $N_{K_d} = 10^{-8} \text{ M}$.

The multimethod KCE toolbox allowed us, for the first time, to determine kinetic parameters of specific and nonspecific protein–DNA interactions. To the best of our knowledge, such a toolbox represents the most powerful approach to kinetic studies of biomolecular interactions.

Discussion and Conclusions

The majority of previous attempts to utilize chromatography and electrophoresis for studying biomolecular interactions were

limited to assuming equilibrium between interacting molecules.^{27,28} Not only does such an assumption limit applications to measuring equilibrium constants, but also this assumption is conceptually mistaken since separation disturbs equilibrium. We state that kinetics must be appreciated when separation methods are used for studies of noncovalent interactions. This appreciation can dramatically enrich the analytical capabilities of the methods.

To prove the benefits of the appreciation of kinetics, we introduce the concept of KCE. Capillary electrophoresis was chosen as a methodological platform as it allows separation in solution (without a solid phase), thus, making kinetic analysis simple and accurate. KCE is defined as the CE separation of molecules that interact during electrophoresis; KCE is not a method but a general concept. To design practical KCE methods, we need to define initial and boundary conditions for interactions. The first KCE methods, NECEEM and SweepCE, were “discovered” by chance. The general concept of KCE provides a “recipe” for rational design of KCE methods. In this work, we used this recipe to define four new KCE methods.

One of the advantages of KCE methods is that mathematical modeling is not necessary for some of them. For example, k_{off} and K_d can be calculated from a single NECEEM electropherogram using trivial formulas, which involve only areas and migration times of peaks.^{8,10} We are currently developing a similar approach for ppKCE, which will allow the finding of both k_{on} and k_{off} from a single electropherogram using simple formulas without the nonlinear regression analysis. Another example of such an “easy-math” application of KCE methods is selection of aptamers with predefined binding parameters.^{17,29} These applications of KCE methods are accessible to researchers with no training in mathematical modeling.

Although expanding the scope of “easy-math” practical applications of KCE methods is important (and is one of our primary goals), the role of mathematical modeling in KCE is difficult to overestimate. Deriving “easy” formulas is very challenging and can be impossible for many KCE methods. To facilitate a generic approach to analyzing KCE data, we developed a multigrid algorithm for numerical modeling of KCE electropherograms. The multigrid algorithm excludes rounding errors, which are typical for modeling chromatographic and electrophoretic data by other numerical methods. The use of a numerical modeling approach allowed us to build a multimethod KCE toolbox for kinetic studies. Different KCE methods have different accuracies for different kinetic parameters. When used together as an integrated tool, KCE methods provide a powerful way of testing hypotheses and accurately calculating binding parameters.

To conclude, we foresee that KCE methods will find multiple applications in fundamental studies of biomolecular interactions, designing clinical diagnostics, and the development of affinity probes and drug candidates. New applications will emerge with further development of KCE.

- (27) Chu, Y. H.; Avila, L. Z.; Biebuyck, H. A.; Whitesides G. M. *J. Med. Chem.* **1992**, *35*, 2915–2917.
 (28) Heegaard, N. H. H.; Nissen, M. H.; Chen, D. D. Y. *Electrophoresis* **2002**, *23*, 815–822.
 (29) Drabovich, A.; Berezovski, M.; Krylov, S. N. *J. Am. Chem. Soc.* **2005**, *127*, 11224–11225.

Experimental Section

Chemicals and Materials. Single-stranded DNA-binding protein (SSB) from *E. coli* and buffer components were from Sigma-Aldrich (Oakville, ON). A fluorescently labeled 40-mer DNA nucleotide (FAM-5'-CTTCTGCCCGCTCCTTCCTTCCAACCTTCATCAGCCACC-3') was custom-synthesized by IDT (Coralville, IA). Fused silica capillaries were purchased from Polymicro (Phoenix, AZ). All aqueous solutions were made using Milli-Q quality deionized water and filtered through a 0.22- μm filter (Millipore, Nepean, ON).

Instrumentation. All capillary electrophoresis (CE) procedures were performed using the following instrumentation and common settings and operations unless otherwise stated. CE was carried out with a P/ACE MDQ apparatus (Beckman Coulter, Mississauga, ON) equipped with a fluorescence detector; a 488-nm line of an Ar-ion laser was utilized to excite fluorescence. A 50-cm long (40 cm to the detection window) uncoated fused silica capillary with an i.d. of 75 μm and o.d. of 360 μm was used. The run buffer for electrophoresis was 50 mM Tris-HCl at pH 8.2. The capillary was rinsed with the run buffer for 2 min prior to each run. Electrophoresis was carried out for a total of 10 min by an electric field of 400 V/cm with a positive electrode at the injection end of the capillary; the direction of the electroosmotic flow was from the inlet to the outlet reservoir. The temperature of the capillary and samples was maintained at 20 ± 0.1 °C. At the end of each run, the capillary was rinsed with 0.1 M NaOH for 2 min, followed by a rinse with deionized water for 2 min.

Solutions of SSB and DNA. Solutions of 100 nM SSB and 200 nM DNA as well as equilibrium mixtures (total of 100 nM SSB and 200 nM DNA) were prepared in the CE run buffer (50 mM Tris-HCl, pH 8.2).

NECEEM. The inlet and outlet reservoirs contained the run buffer, and the capillary was prefilled with the run buffer. A plug of the SSB-DNA equilibrium mixture was injected into the capillary by a pressure pulse of $5 \text{ s} \times 0.5 \text{ psi}$; the length and volume of the injected equilibrium mixture were 7 mm and 30 nL, respectively. The ends of the capillary were inserted in the inlet and outlet reservoirs, and the electric field was applied to run electrophoresis.

SweepCE. The capillary was prefilled with the solution of DNA. The inlet reservoir contained the solution of SSB. The outlet reservoir contained the run buffer. The ends of the capillary were inserted in the

inlet and outlet reservoirs, and the electric field was applied to run electrophoresis.

Continuous NECEEM (cNECEEM). The outlet reservoir contained the run buffer, and the capillary was prefilled with the run buffer. The inlet reservoir contained the SSB-DNA equilibrium mixture. The ends of the capillary were inserted in the inlet and outlet reservoirs, and the electric field was applied to run electrophoresis.

Short SweepCE (sSweepCE). The capillary was prefilled with a solution of DNA. The inlet and outlet reservoirs contained the run buffer. A plug of the SSB solution was injected into the capillary by a pressure pulse of $5 \text{ s} \times 0.5 \text{ psi}$; the length and volume of injected plug were 7 mm and 30 nL, respectively. The ends of the capillary were inserted in the inlet and outlet reservoirs, and the electric field was applied to run electrophoresis.

Plug-Plug KCE (ppKCE). The inlet and outlet reservoirs contained the run buffer, and the capillary was prefilled with the run buffer. First, a plug of the DNA solution was injected into the capillary by a pressure pulse of $10 \text{ s} \times 0.5 \text{ psi}$. The length and volume of the plug were 14 mm and 60 nL, respectively. Second, a plug of the SSB solution was injected into the capillary by a pressure pulse of $5 \text{ s} \times 0.5 \text{ psi}$. The length and volume of the plug were 7 mm and 30 nL, respectively. The ends of the capillary were inserted in the inlet and outlet reservoirs, and the electric field was applied to run electrophoresis.

Short SweepCE of Equilibrium Mixture (sSweepCEEM). The inlet and outlet reservoirs contained the run buffer, and the capillary was prefilled with the equilibrium mixture. A plug of the SSB solution was injected into the capillary by a pressure pulse of $5 \text{ s} \times 0.5 \text{ psi}$; the length and volume of injected plug were 3 mm and 6 nL, respectively. The ends of the capillary were inserted in the inlet and outlet reservoirs, and an electric field of 400 V/cm was applied to run electrophoresis.

Numerical Modeling. A computer program for numerical simulation of KCE electropherograms was written in Pascal. Rate constants were determined by nonlinear regression analysis using the minimum chi-square method.

Acknowledgment. This work was supported by Grants from the Natural Sciences and Engineering Research Council of Canada and the Ministry of Economic Development of Ontario.

JA056232L